Surface structured platinum electrodes for the electrochemical reduction of carbon dioxide in imidazolium based ionic liquids

Florin A. Hanc-Scherer[a], Miguel A. Montiel[b], Vicente Montiel[b], Enrique Herrero[b] and Carlos M. Sánchez-Sánchez *[c,d]

Received (in XXX, XXX) Xth XXXXXXXXX 20XX, Accepted Xth XXXXXXXXX 20XX
DOI: 10.1039/b000000x

The direct CO_2 electrochemical reduction on model platinum single crystal electrodes Pt(*hkl*) is studied in $[C_2mim^+][NTf_2^-]$, a suitable room temperature ionic liquid (RTIL) medium due to its moderate viscosity, high CO_2 solubility and conductivity. Single crystal electrodes represent the most convenient type of surface structured electrodes for studying the impact of RTIL ions adsorption in relevant electrocatalytic reactions, such as surface sensitive electrochemical CO_2 reduction. We propose here based on cyclic voltammetry and in-situ electrolysis measurements, for the first time, the formation of a stable adduct $[C_2mimH\text{-}CO_2^-]$ by a radical-radical coupling after the simultaneous reduction of CO_2 and $[C_2mim^+]$. It means between the CO_2 radical anion and the radical formed from the reduction of the cation $[C_2mim^+]$ before forming the corresponding electrogenerated carbene. This is confirmed by the voltammetric study of a model imidazolium-2- carboxylate compound formed following the carbene pathway. The formation of that stable adduct $[C_2mimH\text{-}CO_2^-]$ blocks CO_2 reduction after a single electron transfer and inhibits CO_2 and imidazolium dimerization reactions. However, the electrochemical reduction of CO_2 under those conditions provokes the electrochemical cathodic degradation of the imidazolium based RTIL. This important limitation in CO_2 recycling by direct electrochemical reduction is overcome by adding a strong acid, $[H^+][NTf_2^-]$, in solution. Then, protons become preferentially adsorbed on the electrode surface by displacing the imidazolium cations and inhibiting their electrochemical reduction. This fact allows the surface sensitive electro-synthesis of HCOOH from CO_2 reduction in $[C_2mim^+][NTf_2^-]$, being Pt(110) the most active electrode studied.

Introduction

Carbon dioxide (CO_2) emissions arising from human activity are considered as a major contributor to the global greenhouse effect. Thus, the CO_2 conversion into useful chemical products and/or energy is a critical concern nowadays.[1] CO_2 reduction can yield a large variety of useful products, such as C_1 species like carbon monoxide (CO), formic acid (HCOOH), methane (CH_4) and methanol (CH_3OH), or C_2 products like oxalic acid ($H_2C_2O_4$), ethane (C_2H_6), ethanol (C_2H_5OH), and ethylene (C_2H_4). Indeed, different alternatives have been studied to transform CO_2,[2,3] which include electro-synthesis of pharmacological or industrial valuable compounds,[4,5] chemical reduction by heterogeneous catalysis,[6,7] photocatalytic conversion,[8,9] and electrochemical reduction, which comprises molecular catalysed electrochemical reduction of CO_2[10-12] and direct electrocatalytic reduction of CO_2.[12-16]

In particular, direct electrochemical conversion and recycling of CO_2 represents a promising pathway, where product selectivity strongly depends on two main factors; (*i*) the electrode material employed[13,15] and (*ii*) the nature of the solvent (aqueous/non-aqueous) supporting electrolyte system.[14,17] The type of solvent is an important factor for the electrochemical CO_2 reduction, since most studies in aqueous media present some difficulties to control the concomitant side reaction of hydrogen evolution which takes place at similar thermodynamic potentials.[18] On the other hand, conventional aprotic non-aqueous media such as, dimethyl sulfoxide (DMSO), N,N-dimethyl formamide (DMF) or acetonitrile (AN), present several advantages, since they avoid hydrogen evolution and present high CO_2 solubility (see Table 1). However, their main drawbacks are their high toxicity and volatility, the costly electrolytes employed and the difficulty for recycling the solvent and the electrolyte. A special category of non-aqueous solvents is comprised by the room-temperature ionic liquids (RTILs), which have been pointed out as the most suitable solvents for carrying on the future developments in electrochemistry.[19] RTILs are commonly defined as materials composed entirely of organic cations and organic or inorganic anions, which melt at or below 100°C.[20] This low melting point is their main difference versus molten salts, which require high working temperatures. Moreover, RTILs present a unique set of properties, which includes suitable ionic conductivity, high thermal stability, negligible vapor pressure and

non-flammability.[21] All these properties allow RTILs to perform simultaneously the role of solvent and electrolyte in electrochemical applications and rule out any safety concern. RTILs comprise a large number of different solvents, but depending whether the cation employed presents an available proton or not, two main subdivisions are possible; protic ionic liquids (PILs)[22] and aprotic ionic liquids (AILs).[23] Imidazolium based cations represent an example of that, since depending on the degree of substitution within the imidazolium ring they belong either to the PILs (1,2-dialkyl-imidazoliums) or AILs (1,3-dialkyl-imidazoliums and 1,2,3-trialkylimidazoliums). One of the major drawbacks of RTILs in electrochemical applications is their high viscosity, since this produces low diffusion of the electroactive species and limits the maximum current density in the process. The RTILs viscosity varies with the type of cation and anion. In particular, 1,3-dialkyl-imidazolium [$C_n mim^+$] cations are one of the most common RTIL cations for electrochemical purposes, since they exhibit both high ionic conductivity and low viscosity values in comparison with all other RTIL cations. Conductivity and viscosity are inversely related, being the alkyl chain length (n) on the imidazolium cation responsible for limiting both. For this reason, the short alky chain (n=2) cation, 1-ethyl-3-methylimidazolium [$C_2 mim^+$], presents both low viscosity and high conductivity values and is selected as a suitable solvent in the present work. This cation is combined with an asymmetric anion like bis(trifluoromethylsulfonyl)imide [NTf_2^-], which also presents one of the lowest viscosity values among most common anions in RTILs.[21] Thus, [$C_2 mim^+$][NTf_2^-] exhibits a low viscosity (29 cP at 298 K)[21] combined with a high solubility of CO_2, comparable to the one exhibited in non-aqueous solvents (see Table 1). In principle, the gas solubility in RTILs is mainly controlled by the nature of the RTIL anion. Thus, a strong interaction of CO_2 with the RTIL anion is the best indicator of CO_2 solubility, being [NTf_2^-] the anion presenting one of the greatest affinity for CO_2.[24] Moreover, this hydrophobic anion allows [$C_2 mim^+$][NTf_2^-] to be water immiscible, which is an advantage, since the water solubility in [$C_2 mim^+$][NTf_2^-] limits its available electrochemical window (3400 ppm H_2O in atmospheric conditions at 298 K).[25] For all those reasons, its moderate viscosity, high CO_2 solubility and conductivity, we propose herein [$C_2 mim^+$][NTf_2^-] as the suitable RTIL for studying the direct CO_2 electrochemical reduction on model surfaces such as platinum single crystal electrodes.

Table 1. CO_2 solubility and viscosity of different solvents at 298 K.

Solvent	Solubility (M)[26-28]	Viscosity (cP)[21]
H_2O	0.033	(0-1)
Acetonitrile (AN)	0.279	(0-1)
[$C_2 mim^+$][NTf_2^-]	0.130	29

After solvent selection, the other key point controlling the product selectivity in the electrochemical reduction of CO_2 is the electrocatalytic activity of the electrode material. Thus, the interaction of CO_2 with the metal surface in the presence of [$C_2 mim^+$][NTf_2^-] ionic pairs. In spite of that, only a few reports have approached that interaction pointing out structures such as the checkerboard-type sandwich arrangement with imidazolium cations and [NTf_2^-] anions absorbed alternatively next to each other on the electrode substrate.[29,30] For this reason, single crystal electrodes represent the most convenient type of surface structured electrodes for studying the impact of RTIL ions adsorption in electrocatalytic reactions, since they provide site distribution control at the electrode surface. In particular, we propose studying the electrocatalytic activity for CO_2 reduction as a function of surface sites using Pt single crystal (Pt(*hkl*)) electrodes, since it has been already proved that imidazolium cation adsorption is a surface-sensitive process[31] and this may drastically affect the CO_2 reduction activity at the electrode.

Electrochemical reduction of CO_2 on Pt(*hkl*) electrodes in acid aqueous solution takes place at potentials where hydrogen adsorption also occurs. Moreover, this reaction presents high sensitivity towards the surface site available at the electrode surface by displaying low activity at highly ordered Pt(111) and Pt(100), but high activity at Pt(110), kinked and stepped surfaces.[32-34] More recently, several Pt(*hkl*) electrodes selectively modified with adsorbed adatoms (Bi, Te and Sb) have also exhibited high catalytic activity for CO_2 reduction in buffered neutral aqueous media.[16] In contrast, electrocatalytic studies for CO_2 reduction in different RTILs have been only reported using Pt polycrystalline surfaces.[35,36] But, as far as the authors knowledge, the electrochemical reduction of CO_2 on Pt(*hkl*) electrodes in a RTIL medium has not been reported yet. Only a few articles devoted to study conducting polymers[37] or electrochemical hydrogen[38,39] and carbon monoxide[40] oxidation reactions on Pt(*hkl*) electrodes in different RTILs can be found in the literature.

It is well established in the electrocatalytic CO_2 reduction reaction that the first reaction step consists in the CO_2 adsorption at the electrode surface and the subsequent electron transfer to form the corresponding radical-anion ($CO_2^{\bullet-}$), as is described in scheme 1, where M stands for the metal electrocatalyst.[15] Moreover, in liquid electrolytes it has been also described that CO_2 may form adducts by coupling with different anions present in solution, such as BF_3Cl^- or 1-isoquinolinecarboxylic acid.[35,41] The formation of those adducts weakens the C=O bond and makes the reduction of CO_2 more favorable. For this reason, it has been recently suggested that a convenient way to lower the potential necessary for achieving the first electron transfer for CO_2 reduction is decreasing the $CO_2^{\bullet-}$ free energy of formation. This is achieved by forming a complex between the $CO_2^{\bullet-}$ and an imidazolium based cation such as [$C_2 mim^+$], since this will help to decrease the overall energy barrier.[42] The formation of such a complex has been proposed as the main responsible for the highly active ionic-liquid mediated electrochemical conversion of CO_2 to CO at low overpotentials in a mixture of water and an imidazolium based ionic liquid. After the first electron transfer forms $CO_2^{\bullet-}$, several possible reaction pathways may be followed depending on the solvent conditions. They can be mainly divided in those that need abundant presence of available protons and a second electron transfer, which may form either HCOOH (scheme 2), if the proton is attached to the $CO_2^{\bullet-}$, or CO (scheme 3), if the proton removes one of the oxygen atoms within the $CO_2^{\bullet-}$. In contrast, if protons are not available, as usually happens in nonaqueous systems, the dimerization reaction mainly produces $C_2O_4^{2-}$ (scheme 4).

$$M + CO_2 + e^- \longrightarrow M\cdots CO_2^{\bullet -} \quad (1)$$

$$CO_2 + 2H^+ + 2e^- \longrightarrow HCOOH \quad (2)$$

$$CO_2 + 2H^+ + 2e^- \longrightarrow CO \quad (3)$$

$$2CO_2 + 2e^- \longrightarrow C_2O_4^{2-} \quad (4)$$

Experimental

Chemicals and electrodes

The ionic liquid 1-ethyl-3-methylimidazolium bis(trifluoromethylsulfonyl) imide [C_2mim$^+$][NTf_2^-] 98% was supplied by Aldrich. This was used straight from the supplier, its water content was minimized by keeping it under argon atmosphere within a silica gel container. The 1,3-dimethylimidazolium-2-carboxylate ($C_6H_8N_2O_2$) > 80% was supplied by Aldrich. The bis(trifluoromethanesulfonyl) amine [H^+][NTf_2^-] 95% supplied by Aldrich is a strong acid, which is fully dissociated when is dissolved in [C_2mim$^+$][NTf_2^-]. Ar and CO_2 ≥ 99.998 purity supplied by Air Liquide were used in all experiments.

Pt polycrystalline electrode and Pt (100), Pt (110) and Pt (111) single crystal electrodes[43] were made from single crystal platinum beads (2.5 mm in diameter), obtained by fusion and subsequent slow crystallization of a 99.999% platinum wire (0.5 mm in diameter). For the Pt(*hkl*) electrodes, after careful cooling, the resulting single crystal beads were oriented, cut and polished following the procedure described by Clavilier *et al.* in.[44] Prior to any experiment, the Pt(*hkl*) electrodes were air flame-annealed[45] for 20-30 s, cooled in a reductive atmosphere (H_2:Ar, ratio 1:3 v/v), quenched in [C_2mim$^+$][NTf_2^-] in equilibrium with that atmosphere and finally immersed in the electrochemical cell under potential controlled conditions using a meniscus configuration.

Electrochemical characterization

A one compartment electrochemical glass cell with a three-electrodes configuration at room temperature and atmospheric pressure was employed for performing cyclic voltammetry experiments. All measurements were made using a computer controlled Autolab PGSTAT30 potentiostat driven by NOVA software. The electrocatalytic activity for the CO_2 reduction reaction was studied in the presence and the absence of a proton source using [C_2mim$^+$][NTf_2^-] as a solvent supporting electrolyte system. Prior to any experiment, the electrochemical cell was dried in hot air and Ar gas was flowed into the empty cell in order to remove any trace of water. A small volume of [C_2mim$^+$][NTf_2^-] (~3.5 mL) was used in each experiment and this was saturated with either Ar or CO_2 gas for at least 20 min before each experiment. A platinum wire, 0.5 mm diameter, was used as a counter electrode and the reference electrode was also another Pt wire electrode (quasi-reference electrode). This reference was placed inside of a glass cylinder with a glass frit separator at the bottom and immersed in a solution identical to the one initially used within the electrochemical cell. This is necessary to isolate the quasi-reference electrode as much as possible from potential chemical interferences derived from the faradic processes occurring in solution during cyclic voltammetry.[46] This is a crucial issue here, since the highly negative potentials reached in voltammetries may provoke H_2 evolution in some extension, which in contact with the Pt wire quasi-reference electrode may modify its open circuit potential and subsequently, the reference potential in the electrochemical cell.

Results and discussion

RTILs generally exhibit a wide electrochemical potential window. But, in the absence of any other electroactive species, they may undergo electrochemical degradation. The electrochemical stability of the imidazolium cation limits the cathodic polarization window, since the cation [C_2mim$^+$] may be reduced to form the corresponding radical [C_2mim$^\bullet$]. The carbon atom between the two nitrogen atoms in the imidazolium ring, is the most electron deficient atom and is hence the most active site for reduction as describes Scheme 5.[47]

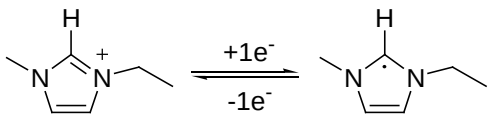

(5)

Figure 1 shows the cyclic voltammogram of [C_2mim$^+$][NTf_2^-] between -1.3 and 1.0 V, where a well-defined quasi-reversible reduction-oxidation response is observed on Pt(111) electrode, which proves high stability for the radical formed [C_2mim$^\bullet$], since this may be oxidized back to the initial cation. This behavior is observed in both, argon and CO_2 saturated [C_2mim$^+$][NTf_2^-]. Similar quasi-reversible voltammograms on Pt(111) electrode were already reported in the literature using several imidazolium-based RTILs.[38] However, if the cathodic limit of potential is extended up to -3.1 V, (Figure 2), this quasi-reversible behaviour disappears. This has been already assigned in the literature to the formation of the corresponding imidazolium carbene by electrochemical reduction and simultaneous hydrogen abstraction following schemes 6[38] or 7.[47-49]

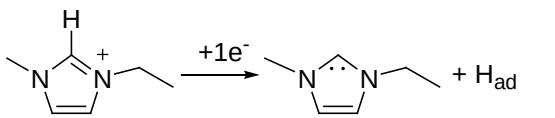

(6)

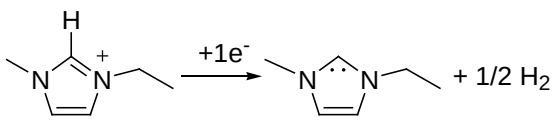

(7)

Furthermore, it is possible to observe in Figure 2 the H_2 evolution reaction in all three low index planes of platinum. Oxidation of the newly formed H_2 can be more clearly observed on Pt(100) and Pt(110) electrodes in the reverse potential scan (inset of Figure 2, oxidation peak between -1.7 and -1.0 V). In contrast, the oxidation peak shown at -0.5 V in Figure 2 has been assigned in the literature[49] to the oxidation of the electrogenerated imidazolium carbene back to the initial cation. In particular, Feroci and co-workers have proposed the use of those electrogenerated imidazolium carbenes as a synthetic tool for capturing CO_2 and forming an imidazolium-2-carboxylate

product by a coupling reaction between the electrogenerated carbene and CO_2 as describes scheme 8.[49,50] This reported reaction takes place outside the electrochemical cell, by CO_2 saturation of $[C_4mim^+][BF_4^-]$ after performing a galvanostatic reductive electrolysis on glassy carbon, Pt, Pd or Au for electrogenerating the corresponding imidazolium carbene. This CO_2 coupling reaction is reported to produce a diminution in the oxidation current at -0.5 V assigned to the carbene oxidation back to the initial cation when the voltammogram in CO_2 presence is compared with the one in CO_2 absence, since most of the carbene is consumed by reaction with CO_2. For this reason, the imidazolium-2-carboxylate product formed in scheme 8 is reported as an electroinactive adduct,[49] which may only give back CO_2 and imidazolium cation by heating induced decomposition.

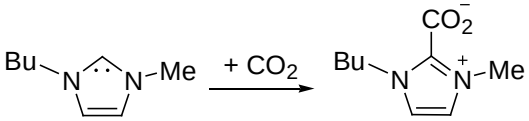

(8)

In contrast, when we compare the cyclic voltammograms reaching -3.1 V, in the absence of CO_2 in $[C_2mim^+][NTf_2^-]$ (Figure 2) and in CO_2 saturated $[C_2mim^+][NTf_2^-]$ (Figure 3), the oxidation peak current at -0.5 V increases for Pt(110) and Pt(100) in the presence of CO_2, and decreases only for Pt(111), which points out that different processes are taking place. Firstly, H_2 evolution is inhibited in all three Pt(*hkl*) electrodes when CO_2 is present in the electrochemical cell, since no subsequent oxidation current peaks are displayed in the reverse potential scan between -1.7 and -1.0 V (see inset of Figure 3). Secondly, the comparison between the inset in figures 2 and 3 shows an important increase in the oxidation peak current displayed at -0.5 V for Pt(110) and Pt(100) electrodes when CO_2 is present, but none for Pt(111). These facts indicates that the process taking place at potentials more negative than -2.0 V is not only the $[C_2mim^+]$ reduction following schemes 6 or 7. In fact, this corresponds to the simultaneous reduction of $[C_2mim^+]$ and CO_2 species on the Pt(100) and Pt(110) electrodes, which produces the formation of a new stable species $[C_2mimH\text{-}CO_2^-]$ by a radical-radical coupling of both reaction products formed following schemes 1 ($CO_2^{\bullet-}$) and 5 $[C_2mim^{\bullet}]$, as it is globally described in scheme 9 for the first time. In contrast, at Pt(111) electrode, which has been already reported to be less active in acid aqueous solutions for the CO_2 electrochemical reduction,[34] this radical-radical coupling reaction may not take place in $[C_2mim^+][NTf_2^-]$, since -3.1 V is not a cathodic enough potential for significantly reducing CO_2 on Pt(111) following scheme 1. Thus, the reported coupling reaction by Feroci and co-workers between the electrogenerated carbene and CO_2 described in scheme 8 takes place at Pt(111). However, the imidazolium-2-carboxylate formed is electroinactive and for this reason the peak current at -0.5 V decreases in the presence of CO_2 (1.1 mA cm^{-2}) with respect to the absence of CO_2 (1.6 mA cm^{-2}), as described by Feroci *et al.*[49-50] In contrast, the new $[C_2mimH\text{-}CO_2^-]$ adduct described in scheme 9 and formed on Pt(110) and Pt(100) is electroactive and may be easily oxidized back to the initial imidazolium cation at -0.5 V. For this reason, the oxidation peak current for Pt(110) and Pt(100) displayed in the inset of Figure 3 is 2-3 times larger than the one displayed in the inset of Figure 2.

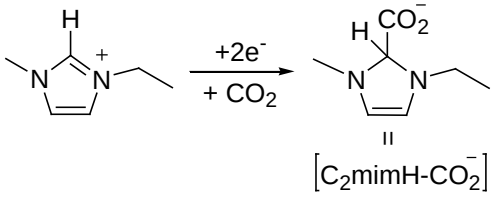

(9)

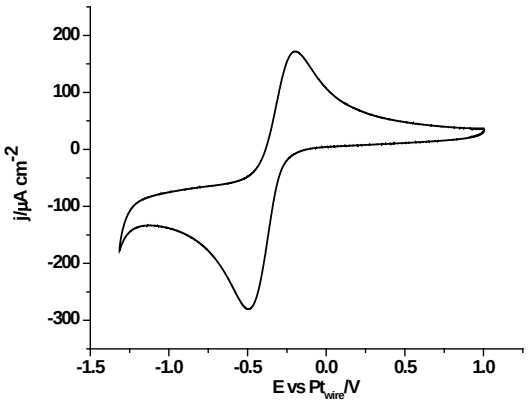

Fig. 1 Cyclic voltammogram of Pt(111) in argon saturated $[C_2mim^+][NTf_2^-]$. Scan rate 0.05 V s^{-1}.

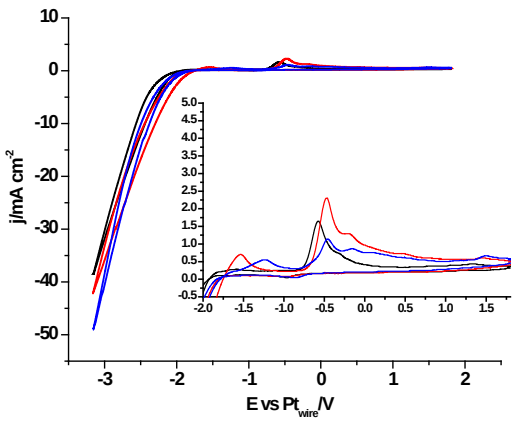

Fig. 2 Cyclic voltammograms of Pt(111), black plot, Pt(110), red plot, and Pt(100), blue plot, in argon saturated $[C_2mim^+][NTf_2^-]$. Scan rate 0.05 V s^{-1}.

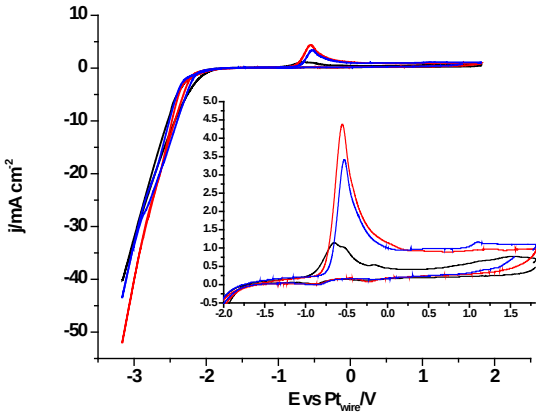

Fig. 3 Cyclic voltammograms of Pt(111), black plot, Pt(110), red plot, and Pt(100), blue plot, in CO_2 saturated $[C_2mim^+][NTf_2^-]$. Scan rate 0.05 V s^{-1}.

Figure 4 shows the electrochemical behaviour of 1,3-dimethylimidazolium-2-carboxylate on Pt polycrystalline electrode as a model carboxylic product of the CO_2 coupling reaction reported in scheme 8. Figure 4 shows the total electroinactivity of that compound within the potential range of interest, from -0.75 V to 1.0 V, in agreement with the literature, since the current density displayed in figure 4 is negligible in comparison with all other voltammograms and no oxidation or reduction peaks appear. This fact demonstrates that the product generated at -3.1 V by simultaneous reduction of $[C_2mim^+]$ and CO_2 at Pt(110) and Pt(100) electrodes does not follow scheme 8 and thus, it is not the imidazolium-2-carboxylate derivate already described in the literature.

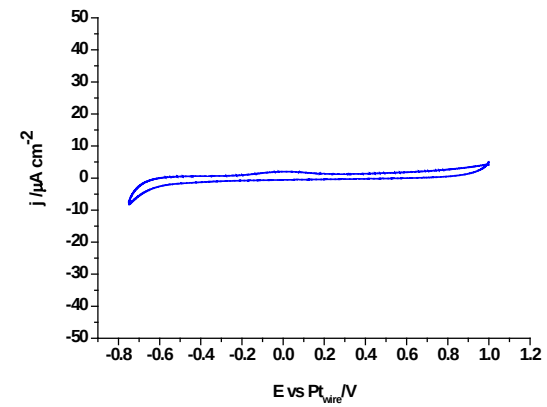

Fig. 4 Cyclic voltammogram of Pt polycrystalline electrode in argon saturated $[C_2mim^+][NTf_2^-]$ containing 50 mM 1,3-dimethylimidazolium-2-carboxylate. Scan rate 0.05 V s^{-1}.

In order to demonstrate that the formation of that new $[C_2mimH\text{-}CO_2^-]$ adduct requires the initial electrochemical reduction of both, $[C_2mim^+]$ and CO_2, as describes scheme 9 and was never proposed before, Figure 5 shows a short in-situ electrolysis at -3.4 V in the presence and the absence of CO_2 followed by a linear voltammogram from -3.4 V to 1.0 V. The peak current at -0.5 V in the argon saturated $[C_2mim^+][NTf_2^-]$ does not increase with the electrolysis time (dashed plot in figure 5), but in the CO_2 saturated $[C_2mim^+][NTf_2^-]$ the peak current at -0.5 V exhibits a constant increase, pointing out a great reversibility of the $[C_2mimH\text{-}CO_2^-]$ adduct for releasing back $[C_2mim^+]$ and CO_2 under oxidative conditions. Thus, the formation of $[C_2mimH\text{-}CO_2^-]$ inhibits radical-radical dimerization reactions to form $C_2O_4^{2-}$ described in scheme 4 as well as the imidazolium radical dimerization reaction.[47,48] However, the electrochemical reduction of CO_2 under those conditions provokes the electrochemical degradation of the imidazolium based solvent and inhibits further electrochemical reduction of CO_2.

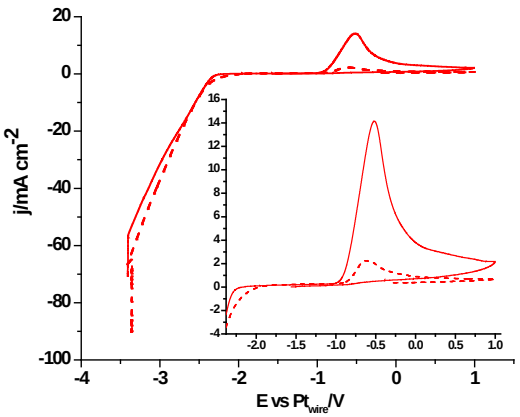

Fig. 5 Linear voltammograms of Pt(110) in $[C_2mim^+][NTf_2^-]$ after holding constant the potential at -3.4 V for 4 min. Dashed red plot, argon saturated and solid red plot, CO_2 saturated solution. Scan rate 0.05 V s^{-1}.

Thus, we think all voltammograms and the in-situ electrolysis reported here demonstrates that the CO_2 reduction in $[C_2mim^+][NTf_2^-]$ is blocked after a single electron transfer and the simultaneous degradation of the imidazolium based solvent is produced by the formation of a stable $[C_2mimH\text{-}CO_2^-]$ adduct. Then, a strong acid as a source of free protons, $[H^+][NTf_2^-]$, is added in solution to facilitate the electrochemical reduction of CO_2 following a 2 electrons pathway to form either HCOOH (scheme 2)[36] or CO (scheme 3)[42]. In the absence of CO_2, Figure 6 displays a clear reduction feature at -1.0 V, corresponding to the reduction of protons to form H_2 at the Pt(*hkl*) electrode surface and its corresponding reversible oxidation on the reverse potential scan.[38] This process seems to inhibit the $[C_2mim^+]$ reduction, because no reduction peak is shown at -0.5 V. Thus, the electrode-RTIL interface has been drastically modified by the presence of a high concentration of available protons, which are preferentially adsorbed and have displaced the imidazolium cations from the surface of the electrode, catalyzing the proton reduction and inhibiting the $[C_2mim^+]$ reduction.

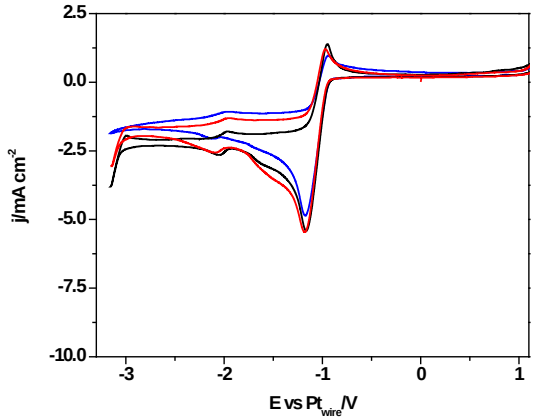

Fig. 6 Cyclic voltammograms of Pt(111), black plot, Pt(110), red plot, and Pt(100), blue plot. Solution composition 270 mM $[H^+][NTf_2^-]$ in argon saturated $[C_2mim^+][NTf_2^-]$. Scan rate 0.05 V s^{-1}.

In contrast, figure 7 exhibits the voltammetric profiles in the presence of dissolved CO_2 and protons with different lower potential limits. When the lower potential limit is set at -2.5 V (figure 7A), no significant changes are observed in the presence of CO_2 in solution, which indicates that the CO_2 reduction reaction is not taking place. Only when the lower potential limit is set below -3.0 V, changes in the voltammogram are observed, which indicates that CO_2 reduction reaction is taking place. Figures 7B and 7C exhibit a new oxidative peak appeared at 0.3 V, which is univocally linked to the reduction of the CO_2 species present in solution, since this peak is absent in an argon saturated solution (figure 6). This new oxidation peak does not fit our previous findings studying the CO electrooxidation reaction in $[C_2mim^+][NTf_2^-]$, since CO oxidation peak appears at more positive potentials.[40] Furthermore, a very similar peak has been assigned in a recent paper from Compton's group[36] to the oxidation of the HCO_2H/HCO_2^- species formed at a polycrystalline Pt electrode surface after CO_2 reduction in $[C_2mim^+][NTf_2^-]$. Thus, herein we prove that the electro-synthesis of HCOOH from CO_2 reduction in $[C_2mim^+][NTf_2^-]$ is a surface sensitive process, since the three different basal planes of Pt produce different amount of HCOOH, which is denoted by the different peak area displayed in figures 7B and 7C and quantified in Table 2. Thus, the results in Table 2 shows that Pt(110) electrode is the most active basal plane for this reaction and Pt(111) and Pt(100) electrodes exhibit a similar low activity (3 times lower than Pt(110) electrode at -3.5 V).

Table 2. Charge associated to the HCOOH formed by CO_2 reduction, which is quantified by integrating its oxidation peak at 0.3 V in figures 7B and 7C.

Cathodic potential limit (V)	Q (μC cm^{-2}) Pt(110)	Q (μC cm^{-2}) Pt(111)	Q (μC cm^{-2}) Pt(100)
-3.1	15.4	10.8	6.22
-3.5	46.2	14.1	12.9

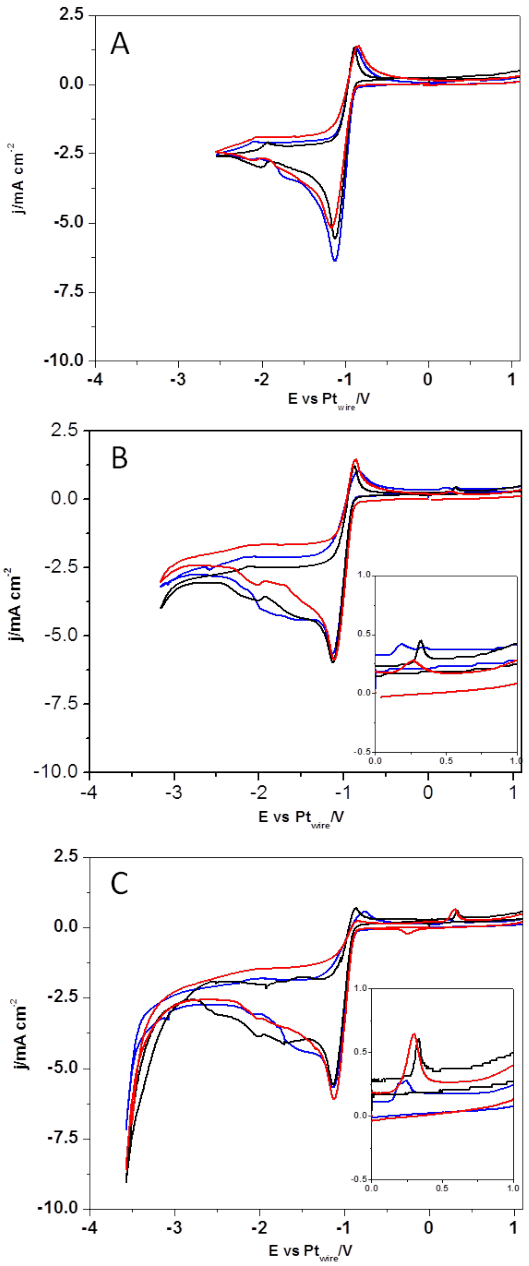

Fig. 7 Cyclic voltammograms of Pt(111), black plot, Pt(110), red plot, and Pt(100), blue plot. Solution composition 270 mM $[H^+][NTf_2^-]$ in CO_2 saturated $[C_2mim^+][NTf_2^-]$. Scan rate 0.05 V s^{-1}. Plots A, B and C represent the same experiment, but reaching a different limit in negative potential: -2.5 V for plot A, -3.1 V for plot B and -3.5 V for plot C.

Conclusions

We study here the direct electrochemical conversion and recycling of CO_2 in one of the most used AILs, the $[C_2mim^+][NTf_2^-]$, which is mainly hydrophobic and presents a suitable set of physical properties for electrochemical purposes such as moderate viscosity, high conductivity and high CO_2 solubility. Moreover, we use Pt single crystal electrodes, which represent the most convenient type of surface structured electrodes for achieving mechanistic information in

electrocatalytic reactions.

We propose, for the first time, the formation of a stable adduct [C_2mimH-CO_2^-] by a radical-radical coupling after the simultaneous reduction of CO_2 and [C_2mim^+]. It means between the CO_2 radical anion and the radical formed from the reduction of the cation [C_2mim^+]. This is especially relevant from a stability point of view, since this reaction provokes the electrochemical degradation of the RTIL employed. So far, only adducts formed by either the reduced form of 1,3-dialkyl-imidazolium cation (carbene) and CO_2,[49,50] bare RTIL anions and CO_2,[35] or the CO_2 radical anion and bare 1,3-dialkyl-imidazolium cation,[42] were previously reported in the literature. However, radical-radical coupling reactions between two 1,3-dialkyl-imidazolium radicals to form a dimer were already reported.[47,48]

We proved by cyclic voltammetry and in-situ electrolysis that is necessary the reduction of both, CO_2 and [C_2mim^+] in order to form the stable adduct [C_2mimH-CO_2^-]. Thus, the formation of such a compound represents an important limitation in the future use of RTILs at industrial scale, since it represents a new cathodic degradation pathway that limits their successful recycling and the extension of the electrochemical CO_2 reduction reaction. Nevertheless, the recyclability of [C_2mim^+][NTf_2^-] and successful direct CO_2 electrochemical reduction is achieved here by adding a proton source [H^+][NTf_2^-] in solution. The presence of protons in high concentration modifies the electrode-RTIL interface by inhibiting the [C_2mim^+] reduction and favoring the HCOOH electro-synthesis. Protons abundance avoids [C_2mim^+] from being adsorbed at the Pt electrode surface and blocks its cathodic degradation.

Finally, we continue increasing the use of RTILs as a safe and non-flammable solvent for studying relevant electrocatalytic reactions from an energetic and environmental point of view. Moreover, we demonstrate that the electrochemical reduction of CO_2 to form HCOOH at the Pt(*hkl*)-RTIL interface remains as a surface sensitive reaction and exhibits the same activity trend than in aqueous acid media by being Pt(110) the most active electrode studied.

Acknowledgements

This work has been partially financed by Generalitat Valenciana through Ayudas para la realización de proyectos de I+D para grupos de investigación emergentes (GV/2014/096) and by the MICINN (project CTQ2013-48280-C3-3-R). Dr. Hanc-Scherer thanks his former supervisor Prof. Petru Ilea for his advice.

Notes and references

[a] *Babes-Bolyai University, Faculty of Chemistry and Chemical Engineering, 11 Arany Janos Street, RO-400028 Cluj-Napoca, Romania.*
[b] *Instituto Universitario de Electroquímica, Universidad de Alicante, Ap. 99, 03080, Alicante, Spain.*
[c] *Sorbonne Universités, UPMC Univ Paris 06, UMR 8235, Laboratoire Interfaces et Systèmes Electrochimiques, F-75005, Paris, France.*
[d] *CNRS, UMR 8235, LISE, F-75005, Paris, France. Fax: 33 144274074; Tel: 33 144274158; E-mail: carlos.sanchez@upmc.fr*

References

1 T. Faunce, S. Styring, M.R. Wasielewski, G.W. Brudvig, A.W. Rutherford, J. Messinger, A.F. Lee, C.L. Hill, H. deGroot, M. Fontecave, D.R. MacFarlane, B. Hankamer, D.G. Nocera, D.M. Tiede, H. Dau, W. Hillier, L. Wang, R. Amal, *Energy Environ. Sci.*, 2013, **6**, 1074-1076.
2 E.V. Kondratenko, G. Mul, J. Baltrusaitis, G.O. Larrazábal, J. Pérez-Ramírez, *Energy Environ. Sci.*, 2013, **6**, 3112-3135.
3 T. Sakakura, J.-C. Choi, H. Yasuda, *Chem. Rev.*, 2007, **107**, 2365-2387.
4 B. Batanero, F. Barba, C.M. Sánchez-Sánchez, A. Aldaz, *J. Org. Chem.*, 2004, **69**, 2423-2426.
5 A. Gennaro, C.M. Sánchez-Sánchez, A.A. Isse, V. Montiel, *Electrochem. Commun.*, 2004, **6**, 627-631.
6 Z. Zhang, Y. Xie, W. Li, S. Hu, J. Song, T. Jiang, B. Han, *Angew. Chem. Int. Ed.*, 2008, **47**, 1127-1129.
7 G.A. Olah, A. Goeppert, G.K.S. Prakash, *J. Org. Chem.*, 2009, **74**, 487-498.
8 F. Sastre, A.V. Puga, L. Liu, A. Corma, H. Garcia, *J. Am. Chem. Soc.*, 2014, **136**, 6798-6801.
9 S.C. Roy, O.K. Varghese, M. Paulose, C.A. Grimes, *ACS Nano*, 2010, **4**, 1259-1278.
10 C. Costentin, M. Robert, J.-M. Savéant, *Chem. Soc. Rev.*, 2013, **42**, 2423-2436.
11 C. Finn, S. Schnittger, L.J. Yellowlees, J.B. Love, *Chem. Commun.*, 2012, **48**, 1392-1399.
12 R.J. Lim, M. Xie, M.A. Sk, J.-M. Lee, A. Fisher, X. Wang, K.H. Lim, *Catal. Today*, 2014, **233**, 169-180.
13 M. Jitaru, D.A. Lowy, M. Toma, B.C. Toma, L. Oniciu, *J. Appl. Electrochem.*, 1997, **27**, 875-889.
14 C.M. Sánchez-Sánchez, V. Montiel, D.A. Tryk, A. Aldaz, A. Fujishima, *Pure Appl. Chem.*, 2001, **73**, 1917-1927.
15 R.P.S. Chaplin, A.A. Wragg, *J. Appl. Electrochem.*, 2003, **33**, 1107–1123.
16 C.M. Sánchez-Sánchez, J. Souza-Garcia, E. Herrero, A. Aldaz, *J. Electroanal. Chem.*, 2012, **668**, 51-59.
17 F. Zhou, S. Liu, B. Yang, P. Wang, A.S. Alshammari, Y. Deng, *Electrochem. Commun.*, 2014, **46**, 103-106.
18 M. Gattrell, N. Gupta, A. Co, *J. Electroanal. Chem.*, 2006, **594**, 1-19.
19 M. Armand, F. Endres, D.R. MacFarlane, H. Ohno, B. Scrosati, *Nat. Mater.*, 2009, **8**, 621-629.
20 N.V. Plechkova, K.R. Seddon, *Chem. Soc. Rev.*, 2008, **37**, 123-150.
21 *Topics in Current Chemistry, Ionic Liquids*, ed. B. Kirchner; Springer, Heidelberg, 2010, Vol. 290.
22 T.L. Greaves, C.J. Drummond, *Chem. Rev.*, 2008, **108**, 206-237.
23 P. Hapiot, C. Lagrost, *Chem. Rev.*, 2008, **108**, 2238-2264.
24 C. Cadena, J.L. Anthony, J.K. Shah, T.I. Morrow, J.F. Brennecke, E.J. Maginn, *J. Am. Chem. Soc.*, 2004, **126**, 5300-5308.
25 A.M. O'Mahony, D.S. Silvester, L. Aldous, C. Hardacre, R.G. Compton, *J. Chem. Eng. Data*, 2008, **53**, 2884-2891.
26 K. Ohta, M. Kawamoto, T. Mizuno, D.A. Lowy, *J. Appl. Electrochem.*, 1998, **28**, 717-724.
27 A. Gennaro, A.A. Isse and E. Vianello, *J. Electroanal. Chem.*, 1990, **289**, 203-215.
28 S.S. Moganty, R.E. Baltus, *Ind. Eng. Chem. Res.*, 2010, **49**, 5846–5853.
29 H.-P. Steinrück, P. Wasserscheid, *Catal. Lett.*, 2015, **145**, 380-397.
30 Y.-Z. Su, Y.-C. Fu, Y.-M Wei, J.-W. Yan, B.-W. Mao, *ChemPhysChem*, 2010, **11**, 2764-2778.
31 Y.-Z. Su, Y.-C. Fu, J.-W. Yan, Z.-B. Chen, B.-W. Mao, *Angew. Chem. Int. Ed.*, 2009, **48**, 5148-5151.
32 S. Taguchi, A. Aramata, *Electrochim. Acta*, 1994, **39**, 2533-2537.
33 N. Hoshi, S. Kawatani, M. Kudo, Y. Hori, *J. Electroanal. Chem.*, 1999, **467**, 67-73.
34 N. Hoshi, Y. Hori, *Electrochim. Acta*, 2000, **45**, 4263-4270.
35 L.L. Snuffin, L.W. Whaley, L. Yu, *J. Electrochem. Soc.*, 2011, **158**, F155-F158.
36 B.C.M. Martindale, R.G. Compton, *Chem. Commun.*, 2012, **48**, 6487–6489.
37 A.P. Sandoval, J.M. Feliu, R.M. Torresi, M.F. Suárez-Herrera, *RSC Adv.*, 2014, **4**, 3383-3391.

38 A.M. Navarro-Suárez, J.C. Hidalgo-Acosta, L. Fadini, J.M. Feliu, M.F. Suárez-Herrera, *J. Phys. Chem. C*, 2011, **115**, 11147-11155.
39 A.P. Sandoval, M.F. Suárez-Herrera, J.M. Feliu, *Electrochem. Commun.*, 2014, **46**, 84-86.
40 F.A. Hanc-Scherer, C.M. Sánchez-Sánchez, P. Ilea, E. Herrero, *ACS Catal.*, 2013, **3**, 2935-2938.
41 C.M. Sánchez-Sánchez, E. Expósito, B. Batanero, V. Montiel, F. Barba, A. Aldaz, *Electrochem. Commun.*, 2004, **6**, 595-599.
42 B.A. Rosen, A. Salehi-Khojin, M.R. Thorson, W. Zhu, D.T. Whipple, P.J.A. Kenis, R.I. Masel, *Science*, 2011, **334**, 643-644.
43 V. Climent, J.M. Feliu, *J. Solid State Electrochem*., 2011, **15**, 1297-1315.
44 J. Clavilier, D. Armand, S.G. Sun, M. Petit, *J. Electroanal. Chem.*, 1986, **205**, 267-277.
45 J. Clavilier, R. Faure, G. Guinet, R. Durand, *J. Electroanal. Chem*., 1980, **107**, 205-209.
46 *Electrochemical Aspects of Ionic Liquids*, ed. H. Ohno, John Wiley and Sons, Hoboken, New Jersey, 2005, pp 30.
47 G.H. Lane, *Electrochim. Acta*, 2012, **83**, 513– 528.
48 N. De Vos, C. Maton, C.V. Stevens, *ChemElectroChem.*, 2014, **1**, 1258-1270.
49 M. Feroci, I. Chiarotto, S.V. Ciprioti, A. Inesi, *Electrochim. Acta*, 2013, **109**, 95-101.
50 M. Feroci, I. Chiarotto, G. Forte, A. Inesi, *J. CO2 Util.*, 2013, **2**, 29-34.